SAND2014-16234J

Mechanisms of Degradation in Adhesive Joint Strength: Glassy Thermoset Polymer Bond in a Humid Environment

Jamie M. Kropka,[*] Douglas B. Adolf,[*] Scott Spangler,[*]
Kevin Austin,[*] and Robert S. Chambers[†]

[*]*Materials Sciences and Engineering Center*
Sandia National Laboratories, Albuquerque, NM 87185-0958

[†]*Engineering Sciences Center*
Sandia National Laboratories, Albuquerque, NM 87185-0346

Abstract

The degradation in the strength of napkin-ring (NR) joints bonded with an epoxy thermoset is evaluated with time in a humid environment. While adherend composition and surface preparation do not affect virgin joint strength, they can significantly affect the role of moisture on the strength of the joint. Adherend surface abrasion and corrosion processes are found to be key factors in determining the reliability of joint strength in humid environments. In cases where surface specific joint strength degradation processes are not active, decreases in joint strength can be accounted for by the glass transition temperature, T_g, depression of the adhesive associated with water sorption. In addition, the decrease in joint strength can be predicted by the Simplified Potential Energy Clock (SPEC) model by shifting the adhesive reference temperature, T_{ref}, by the same amount as the T_g depression. In these cases, joint strength can be rejuvenated to virgin strength by drying. When surface specific degradation mechanisms are active, they can reduce joint strength below that associated with adhesive T_g depression, and joint strength is not recoverable by drying. A critical relative humidity (RH), below which the surface specific degradation does not occur, appears to exist for the polished stainless steel joints.

Sandia National Laboratories is a multi-program laboratory managed and operated by Sandia Corporation, a wholly owned subsidiary of Lockheed Martin Corporation, for the U.S. Department of Energy's National Nuclear Security Administration under contract DE-AC04-94AL85000.

Address correspondence to Jamie M. Kropka, Materials Sciences and Engineering Center, Sandia Corporation, Albuquerque, NM 87185-0985, USA. E-mail: jmkropk@sandia.gov

Keywords: adhesion, degradation, humidity, mechanism

1. Introduction

The performance and reliability of many electrical, mechanical and optical assemblies depend on the integrity of adhesively bonded joints. Unfortunately, the ability to predict the performance of critical polymer-solid interfaces is limited. For instance, cohesive zone modeling techniques for crack growth along a polymer-solid interface typically treat the polymer as an elastic material, a gross simplification that ignores nonlinear relaxations and history dependencies that can have a significant impact on how failure occurs.[1-3] At the same time, interfacial failure analyses using a nonlinear viscoelastic (NLVE) representation of the adhesive,[4-6] which captures nonlinear relaxation and history dependencies, have difficulty defining a failure metric in regions where there are severe strain gradients in the problem, such as at sharp corners. It should be noted that these limitations exist for a freshly bonded, virgin joint. Addressing the reliability of interfacial bonds over time presents even further challenges.

While all of these limitations cannot likely be addressed in a single effort, steps must continue to be made in developing the understanding and tools necessary to predict the performance of polymer bonded interfaces. Over the years, many approaches have been taken to understand adhesion and adhesive joint failure.[7-9] Therefore, it is necessary to clearly define the purpose of the current investigation so that the results can be fit into the context of this history. It is more common to attempt predictions of the propagation of existing surface cracks[10] than to predict the critical traction defining the initiation of de-bonding in an as-designed, un-cracked geometry.[11, 12] The current study attacks the latter problem of assessing the ability of an adhesive interface with no known defects to survive an applied load. The goal is not only to predict the critical traction of a virgin bond, but also to define how that strength changes under environmental exposures. There are certainly many environmental conditions that may affect the strength of a polymer-solid interface, e.g., thermal and strain histories, exposure to small molecules absorbents, etc. Here, we focus on the change of adhesive strength in humid environments, but the testing framework established enables investigations into other environmental influences as well.

The complexity of an adhesively bonded joint makes predicting how it will behave over long periods of time a challenging proposition. For example, failure mechanisms can change with variables such as joint construction and joint history. Considering polymer adhesives bonding metal adherends, the polymer is often the weak-link in the structure if weak interfacial layers[13] are not present. Because of this, work focused on what occurs in the polymer adhesive and how this might be used to predict failure of the bonded joint is of particular interest. In this manuscript, a combination of carefully designed experiments and accompanying finite element stress analyses, with a NLVE representation of the polymer adhesive, are used to resolve adhesive joint failure mechanisms with the ultimate goal of developing a computational approach to predict

failure. The challenges of severe strain gradients in the joint are avoided by intelligent design of the test geometries. Two geometries that fit this criterion include the napkin-ring[3, 14] (NR) and the saucer.[12] In this work, only the napkin-ring joint geometry is used. While the napkin-ring is limited to resolving critical shear tractions, the short diffusion path for moisture through the adhesive makes it attractive for realizing the effects of humid environments on joint strength in relatively short periods of time. The current work set out to address a number of questions. The first was to determine how adherend composition and surface preparation affect the reliability of interfacial bonds over time in humid environments. The results from initial experiments inspired further investigations aimed at answering whether the absorption of water into the adhesive could completely account for the changes in bond strength or whether other factors must be accounted for. Then, both practical application drivers and the desire to further understand the mechanism of joint strength degradation led to experiments designed to resolve whether joint strength could be rejuventated to its virgin value. Initial examinations into the role of relative humidity (RH) on joint strength depression were also carried out. Here, the interest was in determining whether RH just defined the saturation concentration of water absorbed by the adhesive or whether there might be some critical RH level that must be achieved before significant changes in bond strength are resolved.[15] The results of these investigations and current interpretations of the results will be addressed in the following sections of this manuscript.

2. Experimental

The napkin-ring adherends were machined from either 304 stainless steel (304SS) or 6061-T6 aluminum (Al) with dimensions shown in Figure 1(a).

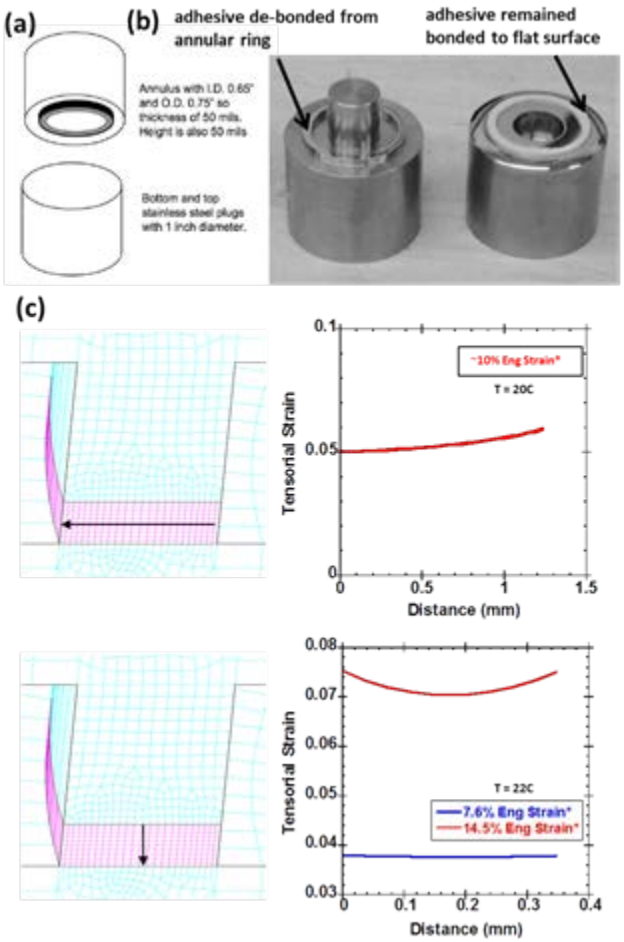

Fig. 1: (a) Schematic of NR geometry, (b) image of NR after failure and (c) shear strain distributions within the adhesive during joint loading. In (c) the pink elements represent the adhesive and the cyan elements represent the adherends, with the annular ring at the top of the adhesive. The arrows illustrate the trace for which local strains are plotted to the right, with the point of the arrow at the largest distance. Tensorial Strain = ½(Eng Strain).

Multiple surface finishes for the annuli and flat plug were examined, including the following: (1) polished (smooth), (2) blasted (rough) with 60 grit red garnet (Barton Mines, ~200 microns), (3) blasted with #39 soda lime glass beads (Crystal Mark, ~50 microns), (4) coated with a chromate primer, BR® 127 (Cytek) and (5) coated with a silane coupling agent, (3-Glycidoxypropyl)trimethoxysilane, GPS (GELEST). All blasting was performed using a Swam-Blast MV-21 (Crystal Mark). Micrographs of the surfaces and a measure of the surface roughness are given in Figure 2.

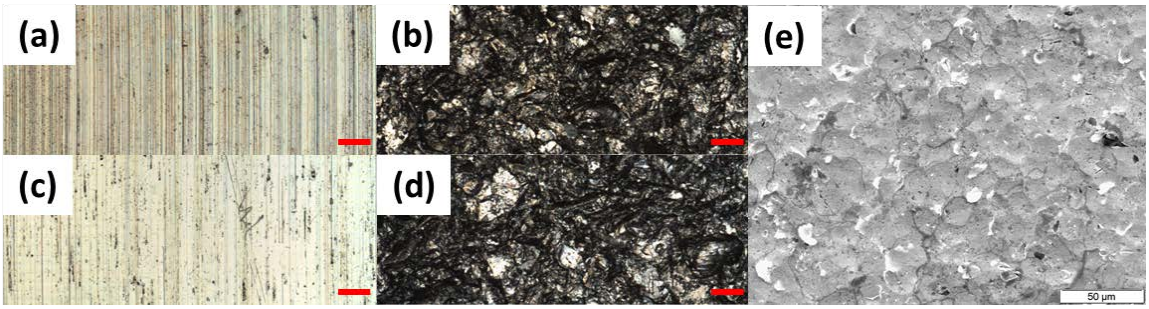

Fig. 2: Surface micrographs of (a) polished 304SS, (b) red garnet blasted 304SS, (c) polished Al, (d) red garnet blasted Al and (e) glass bead blasted 304SS. Red lines on lower part of micrograph represent 50 μm. An Axio CSM 700 confocal microscope (Zeiss) resolved surface roughness, reported as the arithmetic average of the height profile, R_a, as (a) 0.197 μm, (b) 2.02 μm, (c) 0.085 μm and (d) 2.78 μm.

The primer was deposited with flexible swabs, air cured for 30 minutes, and post-cured for 30 minutes at 120^{o}C. The primer thickness was 3 μm, within the manufacturer suggested range 2.5 to 7.5 μm. The glass transition temperature of the primer processed in this manner was measured on a Q2000 differential scanning calorimeter (TA Instruments) to have a midpoint of 115^{o}C during a heating cycle at 10°C/min. The silane coupling agent was added at a level of 2 wt% to a 95 wt% ethanol/ 5 wt% water solution adjusted to pH 4.5-5.5 with acetic acid. A minimum of five minutes was allowed for hydrolysis and silanol formation, after which the adherends were dipped into the solution, agitated gently, and removed after 1-2 minutes. Subsequently, adherends were dipped into ethanol to rinse any excessive deposited material and then cured for 24 hours at room temperature.

Before applying any coatings or bonding the joints, surfaces were cleaned in solvent filled ultrasonic baths (acetone then isopropanol) and blown dry with nitrogen. The adherends were bonded together with the annulus as the upper surface, and the bond line (0.5 mm) was defined by a steel dowel and set-screw that could be backed off after cure to allow frictionless testing. Just after manufacture, all joints were annealed above T_g for 30 minutes and then cooled at 0.5°C/min to room temperature to establish a known history for the viscoelastic adhesive.

After preparation and annealing, some napkin-ring joints were exposed to 60^{o}C and a controlled relative humidity (RH) environment prior to mechanical testing. A bell jar containing de-ionized water, sealed with vacuum grease and vented to the oven, was used to maintain the 100% RH environment. A Z-Plus humidity controlled chamber (Cincinnati Sub-Zero) was used to attain other RH levels. After reaching their equilibrium state in a humid environment, some joints were also dried at 60°C in a desiccated environment.

All joint mechanical loading was completed as a controlled displacement torsional ramp (~ 2% strain/sec) on an Instron 55MT torsional test frame at T=23°C. A minimum of three joints were evaluated at each condition to establish the average stress at failure reported. Error bars denote one standard deviation of the measurements. In the case of aged joints, mechanical testing occurred as soon as possible (within an hour) after removal from the aging condition and equilibrating to the test temperature. For annulus and plug constructed from identical material, de-bonding occurred preferentially at the annulus [see Figure 1(b)] due to the small meniscus formed at the lower, flat plug surface (thereby creating a somewhat larger bonding area). In addition, the stresses and strains within the adhesive during torsional loading of the napkin-ring geometry have been demonstrated to be uniformly distributed [see Figure 1(c)], which enables an experimental determination of the critical shear traction at the point of joint failure.

The adhesive used for testing consisted of the diglycidyl ether of bisphenol A (EPON® Resin 828, Momentive) cured with diethanolamine (DEA, Fisher Scientific) at 12 parts per hundred resin (phr) and hence referred to as 828/DEA. This system exhibits a T_g that is roughly 70°C when cured for 24 hours at 70°C.[16] In addition to using the adhesive to bond napkin-ring joints, thin disk samples, diameter (d) ~ 1 cm and thickness (l) ~ 160 μm, of the adhesive were also used to quantify water absorption within the material using a Q5000 SA dynamic vapor sorption analyzer (TA Instruments). To do this, samples were first dried at T=60°C and RH=0% to remove residual water from the manufacturing process and then cycled through multiple sorption and desorption cycles. The d/l ratio of approximately 60 enables a 1-D diffusion approximation and evaluation of the diffusion coefficient of water through the adhesive. The T_g of these water saturated adhesive discs was also evaluated on a Q2000 differential scanning calorimeter (TA Instruments) in a heat-cool-heat routine between -50°C and 150°C at 10°C/min. The T_g was evaluated from the heating cycle, taking into account data from the first and second heating cycles.

Finite element stress predictions were performed using the ADAGIO finite element code (in-house software developed at Sandia National Laboratories, NM). ADAGIO is a three-dimensional implicit quasi-statics and dynamics code with a versatile element library, nonlinear material models, large deformation capabilities, and contact. It is built on the SIERRA framework, providing a data management framework for parallel computing. The finite element meshes were generated using …? Define symmetry planes, elements through epoxy thickness, etc. The ADAGIO solutions were obtained through a conjugate gradient algorithm that enforces the momentum balance by minimizing the force residuals. Convergence was defined by requiring the relative residual tolerance to be less than or equal to $1.0E^{-4}$ (based on the ratio of the net residual to the L2 norm of the total reactive force).

Because epoxies are viscoelastic materials with fading memory, it is important to capture their evolving history. Thus all analyses reproduced the history of the

experiments as faithfully as possible. Calculations were initiated at the annealing temperature of 75°C. Samples then were cooled to the test temperature of 23°C at 0.5°C/min, and the thermal residual stresses and strains were computed as the starting state for the imposed mechanical loading. A torsional strain was then applied (how?) at ~2% strain/sec. Joint geometry was idealized, representing the adhesive as a simple annular region with 90 degree corners at the bonding interface. The 828/DEA adhesive was represented with a nonlinear viscoelastic constitutive model, the Simplified Potential Energy Clock (SPEC) model.[6] Other materials were represented as ??.

3. Results and Discussion

The influence of adherend composition and surface preparation on the reliability of adhesive joint strength was first examined by preparing both 304SS and Al napkin-ring joints with multiple surface preparations and exposing the joints to a 100% RH environment at 60°C. The 60°C environment was chosen such that water diffusion into the joint, or any type of activated degradation process, may proceed at an adequate rate while keeping the bonding adhesive below its glass transition temperature, T_g. Joints were periodically removed from this environment, cooled to room temperature, and then a ramped torsional load was applied to failure. The room temperature shear stress at failure is given as a function of exposure time to 100% RH at 60°C in Figure 3.

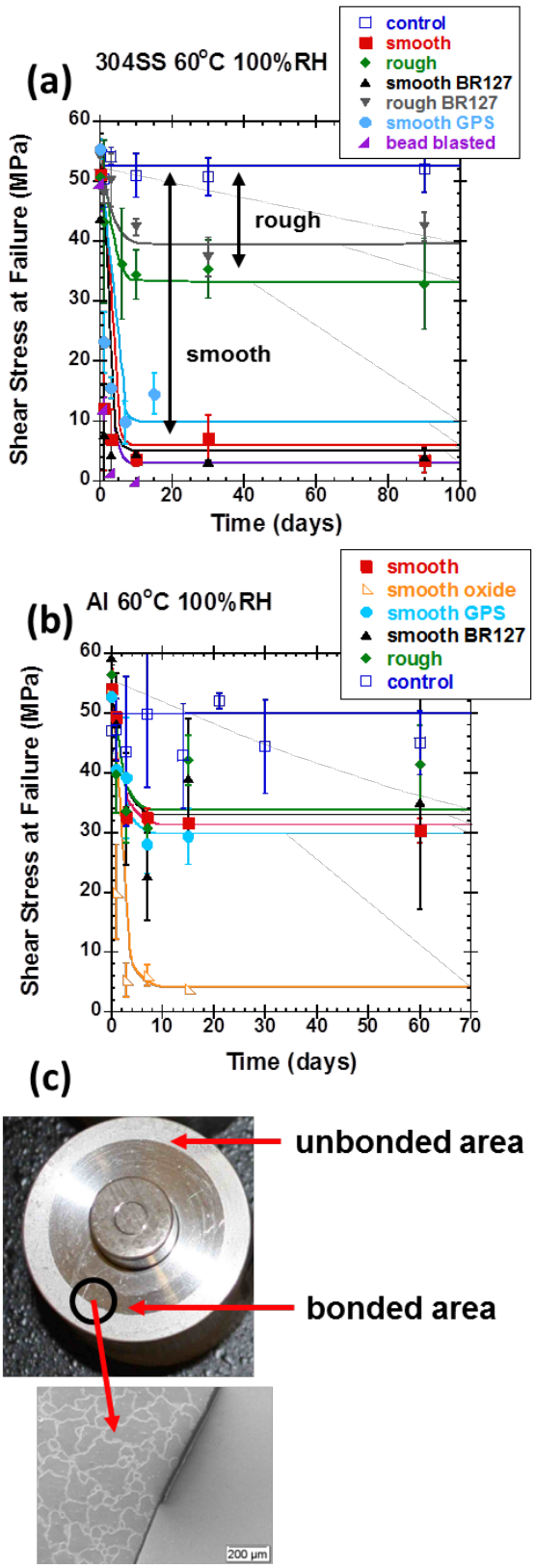

Fig. 3: The time dependence of the shear stress at failure of napkin-ring joints formed from (a) 304SS and (b) Al adherends with various

surface preparations. The lines are just a guide to the eye. Joints were aged at T=60°C and 100% RH (except the control, which was in a dry environment at T=60°C) and tested at room temperature. "Smooth" refers to the polished adherends and "rough" refers to 60 grit red garnet blasted surfaces. The details of these and of the other surface treatments are further explained in the experimental section. "Smooth oxide" refers to polished adherends that exhibited corrosion at the Al-adhesive bonding interface during the environmental exposure. An example of this corrosion on the unbonded area of the joint is given in (c). Why are plug and inner surface of NR not corroded? This region is not sealed from environment.

In Figure 3(a), results are provided for the 304 SS adherends with a number of different surface preparations. The first observation from this plot is that the virgin joint shear stress at failure is independent of surface preparation, even when comparing a polished surface (smooth) to a grit blasted surface (rough). While the independence of joint strength on surface composition and preparation has been reported in tests designed to resolve the critical traction at initiation of joint failure,[3, 12, 17] this is not a universal finding. Indeed, many reports attribute an increase in joint strength with surface roughening to increased bonding area and a "mechanical interlocking" phenomena.[18] Granted, one might anticipate a trade-off between these contributions and stress concentrations, which would exist at sharp features on the rough interface, when it comes to determining how the strength of an interface would change with roughening if a local stress-based criterion for failure is assumed. This trade-off, along with other potential explanations for changes in joint strength associated with surface roughening have been discussed elsewhere[12, 19] and will not be further examined here. For the napkin-ring joint, the independence of virgin joint strength on surface preparation may well be associated with the mechanism of failure in the joint. The temperature dependence of the experimental shear stress at failure for the napkin-ring joint coincides with the temperature dependence of the predicted shear "yield" stress of the adhesive,[12] where polymer adhesive viscoelastic relaxation rates increase to the point that stress decays faster than incremented by the applied ramp. Figure 4 further illustrates the correlation, with multiple adhesives and multiple methods of predicting shear yield.

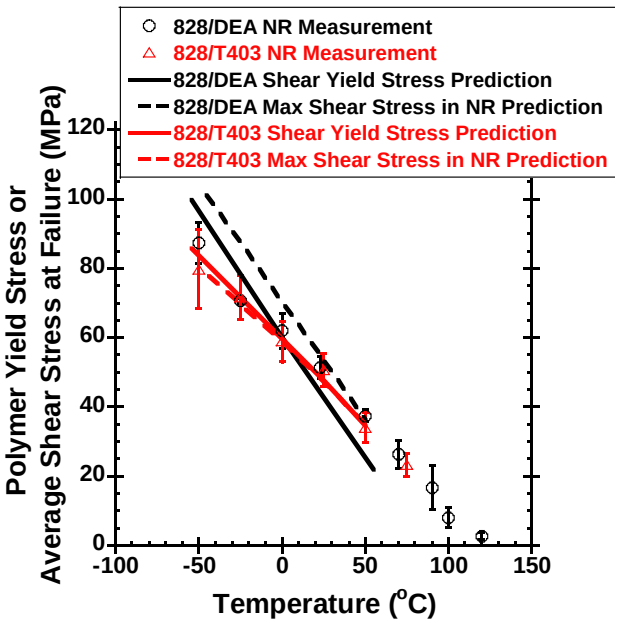

Fig. 4: Experimental shear stress at failure versus temperature for napkin-ring joints bonded with 828/DEA and 828/T403, plotted along with SPEC predictions for (1) the adhesive shear yield stress and (2) the maximum stress sustained in a napkin-ring joint under a torsional load. 828/T403 is EPON® Resin 828 (Momentive) cured with Jeffamine® T-403 polyetheramine (Huntsman) at 43 parts per hundred resin. 828/T403 exhibits a T_g of roughly 80°C when fully cured.

This implies that failure of the joint may be initiated by cohesive failure within the adhesive and this could explain the insensitivity of joint strength to surface preparation. If the interfacial shear strength is greater than the cohesive shear strength of the adhesive then joint strength will remain independent of surface composition and preparation unless the changes reduce the interfacial strength below that of the cohesive strength of the adhesive.

Moving on to the time dependence of the shear stress at failure in Figure 3(a), note that the control samples, joints with polished adherends that were exposed to temperatures of 60°C in a desiccated environment, demonstrated no significant change in the shear stress at failure over the three month test period for which they were evaluated. Given that the exposure temperature was close to, but below, the T_g of the adhesive material, physical aging[20] of the adhesive is likely to be significant in these environments. The volume relaxation of the adhesive to a more dense state associated with the physical aging process can result in higher residual stress build-up in the adhesive since confinement at the bonded interfaces does not allow the adhesive to contract as it would like. The volume relaxation process also slows relaxation rates of the adhesive. Any

such effects either cancel each other out or do not have a significant impact on the strength of the joint over the 90 days tested. On the other hand, all joints that experienced the 100% RH appear to equilibrate to a shear stress at failure less than that of the virgin joints. Since the control samples did not exhibit this behavior, the depressed joint strength can be associated with the presence of moisture, not elevated temperature. Further, the magnitude of the equilibrated joint strength is strongly affected by the surface abrasion of the 304 SS adherends. Joints blasted with the red garnet media exhibited equilibrated strengths on the order of ~30-40 MPa, with or without the BR127 primer (the primer was placed on these joints as an exploratory experiment, not because 304SS was anticipated to corrode over the timescale of the experiment). This is significantly below the ~50 MPa strength of the virgin joints but well above the equilibrated strengths of the smooth surface joints, ~5-10 MPa, with or without the BR127 primer and GPS silane coupling agent. Previous work[15] has described abrading aluminum alloy adherends in anticipation of getting rapid changes in joint strength upon exposure to humid environments due to a known poor durability of sandblasted joints. This observation does not seem to hold for the 304SS joints tested here, as the abraded joints appear more durable. The distinction of the dependence of equilibrated joint strength on surface abrasion led to the testing of an additional surface roughening technique, glass bead blasting. Curiously, this surface preparation gave approximately the same result as the smooth, polished surfaces [see Figure 3(a)]. This raises the question as to what the key factor in determining the equilibrated strength is. Could it be surface topology, surface chemistry (which could change if blast media remains embedded in the adherend surface), or some combination of multiple effects? The answer to this will have to await further investigation. The resulting equilibrated strengths will be further discussed later in this manuscript, but at this point it is already clear that while surface preparation does not have an impact on the virgin strength of the joint it does have an impact on the equilibrated strength of the joint upon exposure to humid environments.

Now focusing on Figure 3(b), where joints constructed from Al adherends are tested in much the same way as the joints constructed of 304 SS adherends in Figure 3(a), some similar and some different observations are made for the time dependence of joint strength in a humid environment (T=60°C and 100% RH). Once again, the virgin joint shear stress at failure is independent of surface preparation and indistinguishable from that of the 304 SS adherend joints. The time dependent data demonstrated much more scatter for the Al adherends than it did for the 304 SS adherends. The root cause of this is not currently known, although many speculations could be made. For now, some statements on the data will be made despite the scatter. The control samples, joints with polished adherends that were exposed to 60°C in a desiccated environment, demonstrated no significant change in the shear stress at failure over the test period. All joints that experienced the 100% RH equilibrated to a shear stress at failure less than that of the

virgin joints. But for the Al adherends, only joints that exhibited a visible corrosion layer growing between the adherend and adhesive equilibrated to strengths of ~5-10 MPa. Some pictures of the corrosion layer growth from these joints are given in Figure 3(c), but no further characterization of this layer has been done to this point. It should be noted that all joints exhibited this growth layer on the Al surface. However, in many cases the epoxy adhesive acted as a primer and prevented corrosion at the bond-line. Bond-line corrosion appears to be necessary to depress joint strength to the ~5-10 MPa level. Humid environments have been shown to convert the oxide layer on Al to an Al hydroxide, which adheres poorly to the metal substrate[21] and leads to a weak boundary layer in the joint.[13] Did these joints fail in the corrosion layer? All other joints equilibrated to strengths of ~30-40 MPa and there was no clear distinction between rough and smooth surfaces as there was for the 304SS joints.

During exposure to T=60°C and 100% RH, the adhesive absorbs water that acts as a plasticizer. To quantify these effects, thin discs of the adhesive were used to track water sorption into the polymer and to evaluate the effect of water sorption on the glass transition of the polymer. The results from these experiments at a number of relative humidity levels at T=60°C are given in Figure 5.

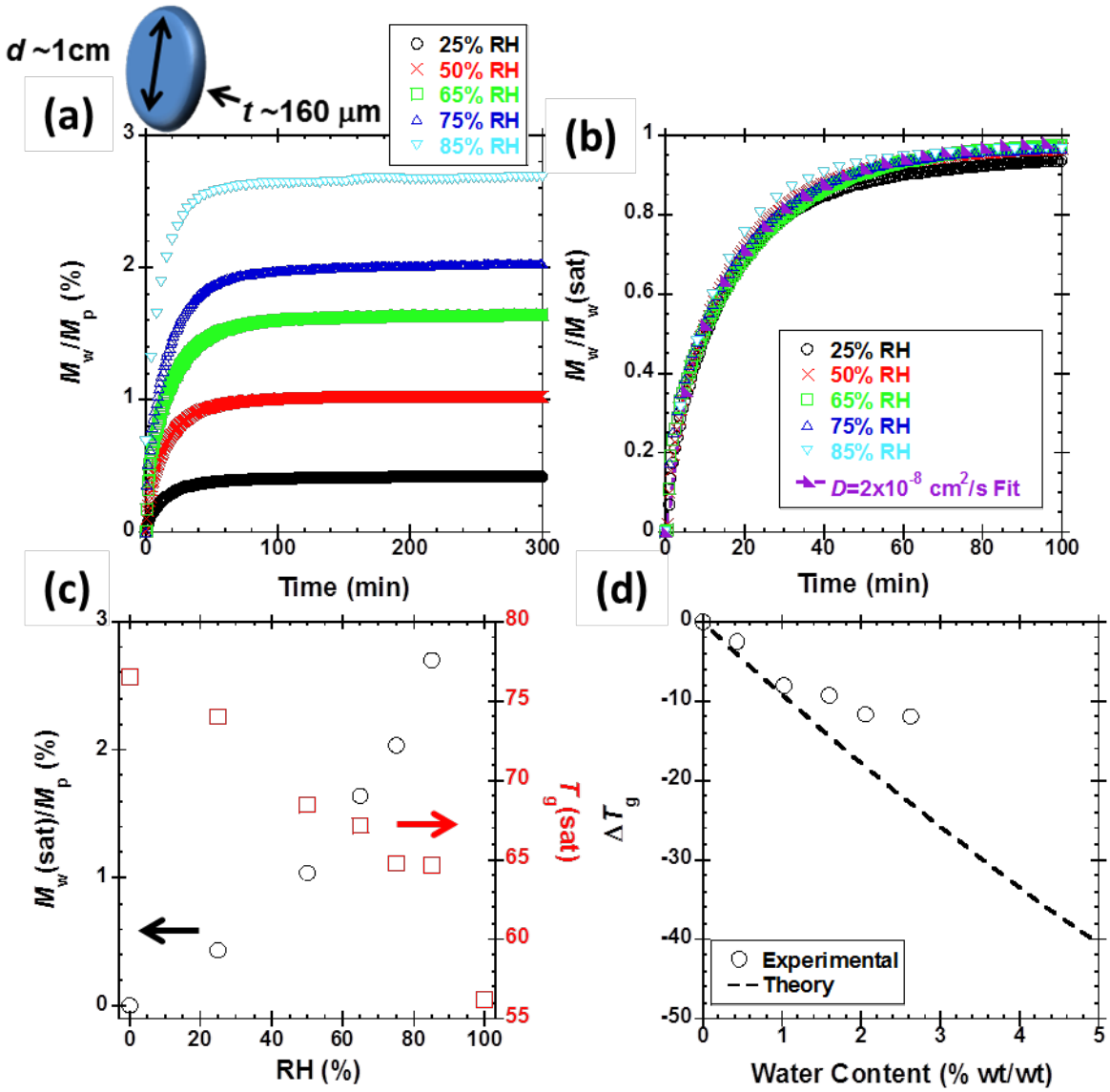

Fig. 5: (a) Adhesive sample geometry and water sorption (tracked as the ratio of the mass of water, M_w, to the mass of polymer, M_p) into the 828/DEA polymer as a function of time at multiple RH, (b) normalization of water sorption by saturation level, M_w(sat), and extraction of a diffusion coefficient, D, through fit to 1-D Fickian diffusion solution, (c) water saturation level and adhesive T_g at saturation as a function of RH and (d) comparison of T_g depression measurements to theoretical[22] predictions. All water sorption data presented was obtained at T=60°C.

From Figure 5(a), both the rate at which water is absorbed and the equilibrium water sorption reached are evident. While not shown, subsequent desorption and absorption

cycles on the same sample were equivalent, and hence no irreversible processes have been observed in these tests. Since 1-D diffusion is applicable in these large aspect ratio samples, a water diffusion coefficient, D, through the polymer can be determined from fits to the 1-D Fickian diffusion solution given in Equation 1,[23, 24]

$$\frac{M_w(t)}{M_w(sat)} = 1 - \frac{8}{\pi^2}\sum_{k\ odd}\frac{e^{-tD\left(\frac{k\pi}{l}\right)^2}}{k^2} \cong 1 - exp\left[-7.3\left(\frac{Dt}{l^2}\right)^{0.75}\right] \qquad \text{Eq. 1}$$

where $M_w(t)$ is the mass of water absorbed into the polymer at time t, $M_w(\text{sat})$ is the mass of absorbed water at saturation, and l is the polymer thickness in the diffusion direction. D is found to be 2×10^{-8} cm^2/s [see Figure 5(b)]. This value is independent of RH and comparable to that observed for water diffusion through other thermoset epoxies.[24, 25] It should be noted that the bulk sorption rate suggests that the napkin-ring joint (assuming 1-D diffusion in the radial direction with a diffusion length, L, of ~0.63 mm) would be water saturated in approximately 3 days ($t\sim L^2/D$), which coincides well with the time it took napkin-ring joint strength to equilibrate (see Figure 3). This could mean that accounting for bulk diffusion may be sufficient (i.e., it may not be necessary to address any potential differences in interfacial diffusion rates[26]) to describe water sorption effects on joint strength. This hypothesis could be tested more rigorously by acquiring more data on napkin-ring joint strength decay within the first three days of exposure to humid environments.

Figure 5(c) shows both the saturated water concentration within the polymer adhesive and the bulk polymer T_g at saturation as a function of the RH level at T=60°C. As anticipated, the absorbed water acts as a plasticizer and depresses the T_g of the bulk polymer. The magnitude of the T_g depression increases with the amount of water absorbed in the polymer. The change in T_g observed with water sorption is compared to theory[22, 27] in Figure 5(d). The theory predicts the T_g of the water imbibed polymer to evolve as in Equation 2,

$$T_{g_{p,w}} = \frac{x_p\Delta C_{pp}^{act}T_{g_p} + x_w\Delta C_{p_w}T_{g_w}}{x_p\Delta C_{pp}^{act} + x_w\Delta C_{p_w}} \qquad \text{Eq. 2}$$

where p and w refer to polymer and the water diluent, respectively, x refers to the weight or mole fraction and ΔC_p^{act} is the incremental change in the specific heat at T_g of the units capable of activation.[28] At water concentrations of 1 wt% and below, the data tracks predictions quite well. At higher water concentration however, experimentally measured changes are less than predicted. Why the measurements deviate from theory has not fully been resolved, but a few comments can be made. First, the glass transition resolved from an initial heating of the sample was greater than or equal to that of a subsequent heating of the same sample. This suggests diffusion of water out of the epoxy during the heating

profile of the calorimeter does not significantly affect the measurement and cause the deviation from theory predictions. If water was diffusing out of the polymer, the glass transition would be anticipated to be higher in the second heating cycle. Diffusion of water out of the polymer at high temperatures would also be anticipated to result in condensation within the sealed sample container upon cooling and a freezing of this condensate at 0°C. In this testing, samples were cooled to -50°C and no sign of water freezing are noted in the calorimetry data. Second, the 828/DEA mixture is epoxide rich and reactive species are known to exist after the cure profile (as observed from an exothermic peak in the calorimeter upon heating the material above the T_g after cure at T=70°C for 24 hours). The reaction of water with the excess epoxide can proceed to form a glycol unit. In addition, the plasticization of the polymer associated with the water absorption has depressed the T_g to approximately the temperature at which the water imbibition was carried out at, 60°C. The reduction of T_g to the material temperature increases mobility in the polymer and the potential for further polymerization reaction. In principal, the effects of any such reactions on the T_g of the polymer can be resolved by evaluating T_g after removing water from the sample. Unfortunately, experiments aimed at this have not resolved clear conclusions. A final experimental comment on this point relates to the potential of physical aging of the sample during the imbibition of water. The water saturated samples were evaluated calorimetrically in a heat-cool-heat temperature ramping scheme between -50°C and 150°C. Differences are noted in the signatures of the glass transition between the first and second heating cycles. The first heating cycle resolves a higher T_g and an enthalpic peak observed as an "overshoot" of the rubbery response of the material above T_g. These are characteristics of physical aging[20] and are erased upon annealing above T_g and reheating the sample in a second thermal scan. The T_g reported here is that from the second scan, with any such physical aging effects removed. Limitations of the thermodynamics-based theory to capture all aspects of the glass transition process may also exist.

Having established the adhesive T_g depression associated with water sorption and that experimental failure of the virgin napkin-ring joint correlates well with the peak shear stress predicted for the napkin-ring geometry by the SPEC nonlinear viscoelastic model, one might ask whether the change in strength in the napkin-ring joints under humid environments could be predicted by the SPEC model by accounting for the change in T_g of the adhesive. Certainly, some assumptions must be made in order to represent the experimental tests with the model. The principal assumption made here is that the change in T_g of the adhesive can be accounted for in the model by simply shifting the reference temperature (the temperature to which shear relaxation data was shifted in order to construct a master relaxation spectrum for the material by time-temperature-superposition), T_{ref}, in the model by the same amount as the T_g depression associated with water sorption. This would imply that the absorption of water does not change the shape

of the polymer relaxation spectrum, it only shifts it by a defined amount that can be accounted for by equating a shift in T_{ref} to the change in the T_g. Model predictions of napkin-ring response with a range of adhesive reference temperatures are given in Figure 6.

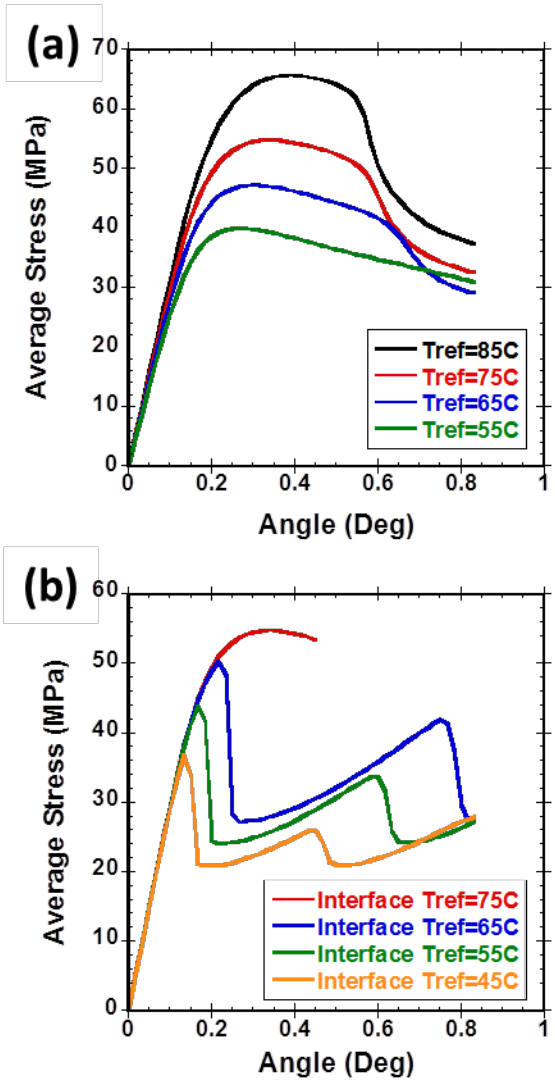

Fig. 6: Finite element model predictions for napkin-ring macroscopic response with change in (a) bulk T_{ref} and (b) an interfacial T_{ref} localized to a 10 μm layer at both adherend boundaries. Average stress in these plots refers to the applied shear force divided by the adhesive-to-adherend bond area. Angle is the rotational displacement applied to the napkin-ring. Predictions are for napkin-ring response at T=23°C with the history described in the experimental section.

Both a bulk [Figure 6(a)] and interfacial [Figure 6(b)] change in the T_{ref} are examined with the model. The latter would be relevant should the water diffuse along the interface at a faster rate than through the bulk. In the case of the interfacial change, T_{ref} is varied in a 10 μm thick interface layer at both adherend boundaries while the T_{ref} in the bulk adhesive is maintained at 75°C. As can be seen in Figure 6, changes in the adhesive T_{ref}, bulk or interfacial, of the magnitude associated with the T_g change experimentally observed with water absorption into 828/DEA can have a significant effect on the maximum predicted shear stress in the joint. Using the maximum predicted shear stress in the napkin-ring as the failure metric, a comparison can be made between predictions and experimental failure loads. This comparison is given in Figure 7.

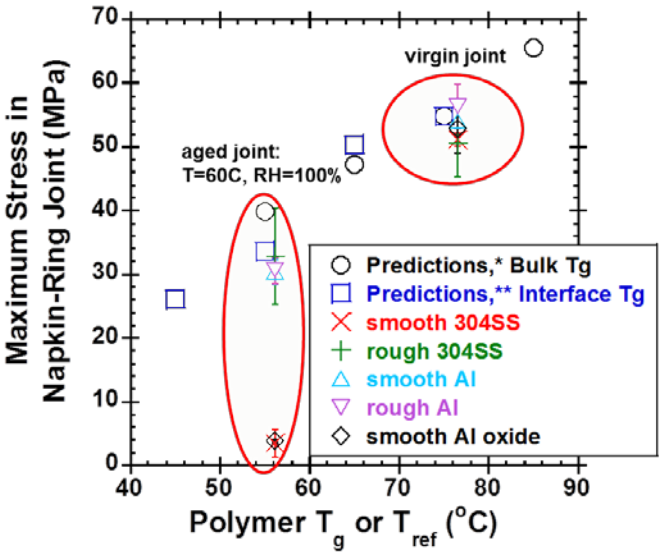

Fig. 7: Maximum stress in napkin-ring joint versus adhesive T_g (experiments) or adhesive T_{ref} (model predictions).

As already shown, the stress at failure in the virgin joint does not vary significantly amongst adherend type or surface preparation and matches closely to the maximum stress predicted in the joint when modeling the adhesive with the SPEC model. The new information in this plot exists in the comparison of joint strength after equilibration at T=60°C and RH=100% to model predictions. Under these conditions the adhesive T_g has been depressed to approximately 55C and many of the joints exhibit a stress at failure between 30 and 40 MPa. This joint strength correlates very closely to the maximum predicted stress in the napkin-ring joint for an adhesive T_{ref} of 55°C, be that the bulk or interfacial T_{ref} of the adhesive. This suggests that the change in joint strength for these

cases can be accounted for by the reduction in adhesive T_g associated with water sorption. To the best of our knowledge, this is the first time that a predictive capability of joint strength has been able to demonstrate a quantitative account of joint strength depression associated with adhesive T_g depression. There are two joint cases, the smooth 304SS and smooth Al oxide, that exhibit a stress at failure much lower than that predicted to be associated with the adhesive T_g reduction. In these cases, other factors must be accounted for that have not been fully elucidated in this work.

Another method to further demonstrate the importance of adhesive T_g depression due to water sorption on the strength of an adhesive joint is to remove the water from the joint and examine whether the strength is rejuvenated. The results of such an experiment are given in Figure 8.

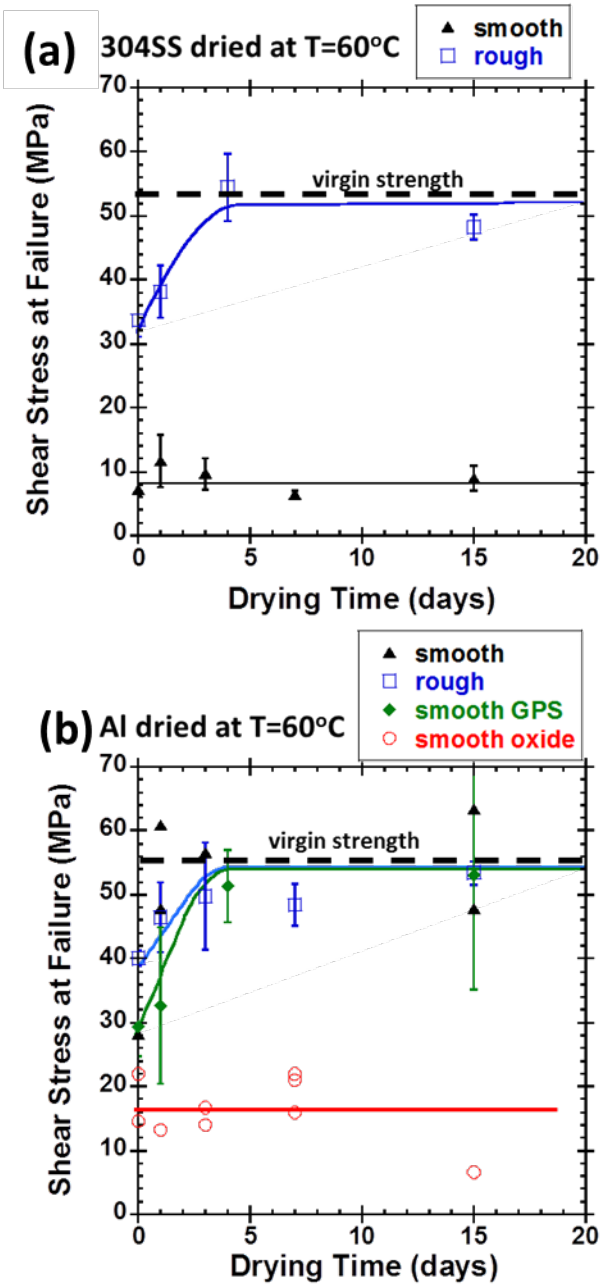

Fig. 8: Napkin-ring shear stress at failure versus time during drying at T=60°C in a dessicated environment (after equilibrating at T=60°C and 100% RH) for (a) 304SS adherends and (b) Al adherends. The lines are just a guide to the eye. In cases with no error bars, individual data points are plotted rather than averages (points) and standard deviations (error bars).

From Figure 8, it is observed that in cases where the drop in joint strength can be accounted for by the depression of the adhesive T_g, joint strength can be fully rejuvenated to the virgin state upon drying. On the other hand, in cases where joint strength drops beyond that associated with adhesive glass transition temperature depression, joint strength is not rejuvenated upon drying. Clearly, in these cases another mechanism is at play that affects joint strength in a non-recoverable way, or at least non-recoverable by heating.

The final results reported here are an examination of the role of relative humidity on the strength of the napkin-ring joint at T=60°C. Only the smooth 304SS adherends were examined under these conditions. These adherends result in joints that exhibited the largest observed effect on adhesive strength at T=60°C and 100% RH and hence provided the best opportunity to experimentally resolve the role of relative humidity on strength at the same temperature. The results of this examination are given in Figure 9.

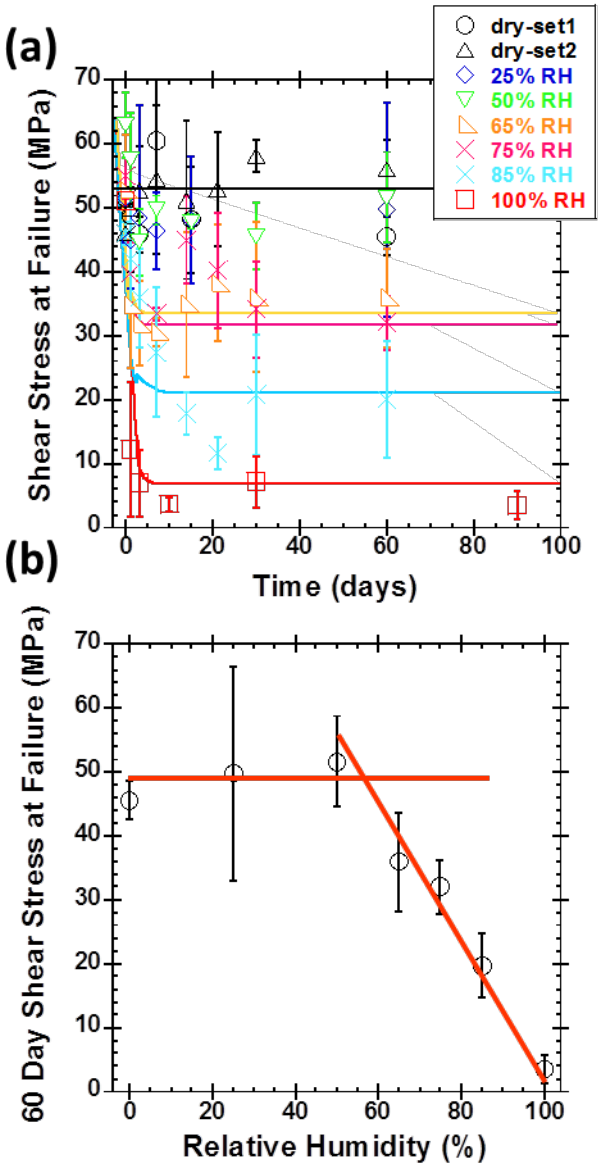

Fig. 9: Smooth 304SS napkin-ring shear stress at failure (a) versus time during exposure to T=60°C and multiple levels of RH and (b) versus RH for joints at T=60°C for 60 days. The lines are just a guide to the eye.

From Figure 9(a), there is no clear change in joint shear stress at failure at 50% RH and below over the 60 day period examined. Above 50% RH, the joint strength drops to lower levels with time and increasing RH. This is further illustrated in Figure 9(b), in which the shear stress at failure of the joint at 60 days is plotted against relative humidity. The lines in Figure 9(b), drawn only as a guide to the eye, are suggestive of a critical humidity, below which adhesive strength does not degrade. The existence of such a

critical humidity has been suggested in previous works.[15, 29, 30] Here, the critical humidity is suspected to be associated with a process that goes on at the adhesive-304SS interface and ultimately reduces the joint strength beyond that associated with water absorption within the adhesive alone. Identification of this process is the focus of current investigations but no conclusions have been drawn from the work to date.

4. Conclusions

In summary, a number of points will be re-emphasized. First, while adherend composition and surface preparation did not have a significant effect on virgin joint debonding stress, these factors do significantly impact the role of moisture on the strength of the joint. For the 304SS adherends, surface abrasion appears to be a defining factor in determining the effect of moisture on the joint strength. For Al adherends, surface abrasion appears to play less of a role in determining the effect of moisture on joint strength, and the corrosion of the bonding interface is what drives joint strength to decrease below that predicted based on adhesive T_g depression associated with water absorption. Interestingly, the addition of primer or silane coupling agent did not result in significant changes in behavior for either adherend.

Considering the correlation between joint failure and SPEC model predictions of maximum shear stress in the napkin-ring, the mechanism of failure in the virgin joint is thought to be run-away nonlinear viscoelasticity(get Bob or Doug to point out the reference that coined this term…also might be better to use and reference it in the result/discussion section first) in the polymer adhesive (i.e., cohesive failure in the adhesive). Changes in adherend composition and surface preparation do not change the locus of failure in the virgin joint and hence joint strength is always defined by the cohesive strength of the polymer. When depression of joint strength in humid environments is fully accounted for by depression of the adhesive T_g due to water absorption, failure remains cohesive in the polymer. However, when joint strength falls below this level, other surface specific phenomena must change the locus of failure to the interface. Understanding what the surface specific phenomena are and how they affect interfacial failure are of interest and continue to be investigated. At this point, these failure mechanisms cannot be accounted for in a predictive technique. More details of specific mechanisms are necessary. The experimentation on joint drying and RH levels do provide some information on the surface specific effects. For instance, the process active in 304SS joints at T=60°C and 100% RH is not reversible upon drying, as observed by the inability to recover joint strength. It also appears that RH must be greater than 50% for the process to occur within 60 days. Unfortunately, these observations cannot pinpoint a specific mechanism. They can only serve to help eliminate some possibilities.

A physically-based path toward predicting the degradation in adhesive strength associated with water sorption into the polymer adhesive for geometries that do not involve severe strain gradients can be envisioned. A model of water influx into the polymer adhesive could be coupled with a SPEC representation of the polymer response to predict runaway nonlinear viscoelasticity. The plasticization and swelling effects of the water on the adhesive must be accounted for, and this may be possible in SPEC in an analogous manner as done to incorporate cure effects.[31] Rigorously coupling diffusion and constitutive response for the multicomponent viscoelastic system may be more complicated.[32, 33] Alternatively, given water diffusion rates and the effect of water on the T_g of the adhesive, maybe an engineering approach would be simpler and sufficient. The best method to examine this would be to work the problem in a rigorous manner and then evaluate where simplifications can be made without losing fidelity in the predictions. We hope to explore this approach in coming years.

Acknowledgements
JMP, WSEAT

References

1. Reedy, E. D., Jr.; Guess, T. R. *J. Adhes. Sci. Technol.* **1996,** 10, (1), 33-45.
2. Liljedahl, C. D. M.; Crocombe, A. D.; Wahab, M. A.; Ashcroft, I. A. *J. Adhes. Sci. Technol.* **2005,** 19, (7), 525-547.
3. Adolf, D. B.; Chambers, R. S.; Hance, B.; Elisberg, B. *J. Adhes.* **2010,** 86, (11), 1111-1131.
4. Caruthers, J. M.; Adolf, D. B.; Chambers, R. S.; Shrikhande, P. *Polymer* **2004,** 45, (13), 4577-4597.
5. Adolf, D. B.; Chambers, R. S.; Caruthers, J. M. *Polymer* **2004,** 45, (13), 4599-4621.
6. Adolf, D. B.; Chambers, R. S.; Neidigk, M. A. *Polymer* **2009,** 50, (17), 4257-4269.
7. Eley, D. D.; Editor, *Adhesion*. Oxford University Press.: 1961; p 290 pp.
8. Gent, A. N.; Hamed, G. R. In *Adhesion and bonding, adhesion*, 1985; Wiley: 1985; pp 476-518.
9. Kinloch, A. J., *Adhesion and Adhesives*. Chapman and Hall: 1987; p 454 pp.
10. Thouless, M. D.; Yang, Q. D. In *Measurement and analysis of the fracture properties of adhesive joints*, 2002; Elsevier Science B.V.: 2002; pp 235-271.
11. Popineau, S.; Shanahan, M. E. R. *Int. J. Adhes. Adhes.* **2006,** 26, (5), 363-370.
12. Adolf, D. B.; Chambers, R. S.; Stavig, M. E.; Kawaguchi, S. T. *J. Adhes.* **2006,** 82, (1), 63-92.
13. Bikerman, J. J., *The Science of Adhesive Joints. 2nd ed*. Academic: 1968; p 349 pp.
14. De Bruyne, N. A.; Houwink, R., *Adhesion and Adhesives*. Elsevier Pub. Co.: 1951; p 517 pp.
15. Brewis, D. M.; Comyn, J.; Raval, A. K.; Kinloch, A. J. *Int. J. Adhes. Adhes.* **1990,** 10, (4), 247-53.
16. http://www.sandia.gov/polymer-properties/828_DEA.html
17. Adolf, D. B.; Stavig, M. E.; Kawaguchi, S.; Chambers, R. S. *J. Adhes.* **2007,** 83, (1), 85-104.
18. Gent, A. N., Hamed, Gary R., Adhesion and Bonding. In *Encyclopedia of Polymer Science and Engineering*, Kroschwitz, J. I., Ed. 1985; Vol. 1, pp 476-518.
19. Jennings, C. W. *J. Adhes.* **1972,** 4, (1), 25-38.
20. Struik, L. C. E., *Physical Aging in Amorphous Polymers and Other Materials*. Elsevier Scientific Publishing Co.: 1978; p 230 pp.
21. Ahearn, J. S.; Davis, G. D.; Sun, T. S.; Venables, J. D. In *Correlation of surface chemistry and durability of aluminum/polymer bonds*, 1983; Plenum: 1983; pp 281-99.
22. Ellis, T. S.; Karasz, F. E. *Polymer* **1984,** 25, (5), 664-9.
23. Crank, J., *The Mathematics of Diffusion. 2d Ed*. Oxford Univ. Press: 1975; p 414 pp.
24. Maggana, C.; Pissis, P. *J. Polym. Sci., Part B: Polym. Phys.* **1999,** 37, (11), 1165-1182.
25. Vanlandingham, M. R.; Eduljee, R. F.; Gillespie, J. W., Jr. *J. Appl. Polym. Sci.* **1999,** 71, (5), 787-798.

26. Linossier, I.; Gaillard, F.; Romand, M.; Nguyen, T. *J. Adhes.* **1999,** 70, (3-4), 221-239.
27. ten Brinke, G.; Karasz, F. E.; Ellis, T. S. *Macromolecules* **1983,** 16, (2), 244-9.
28. Ellis, T. S.; Karasz, F. E.; ten Brinke, G. *J. Appl. Polym. Sci.* **1983,** 28, (1), 23-32.
29. Lefebvre, D. R.; Takahashi, K. M.; Muller, A. J.; Raju, V. R. *J. Adhes. Sci. Technol.* **1991,** 5, (3), 201-27.
30. Cognard, J. *Int. J. Adhes. Adhes.* **1988,** 8, (2), 93-9.
31. Adolf, D. B.; Chambers, R. S. *J. Rheol. (Melville, NY, U. S.)* **2007,** 51, (1), 23-50.
32. Lustig, S. R.; Caruthers, J. M.; Peppas, N. A. *Chem. Eng. Sci.* **1992,** 47, (12), 3037-57.
33. Kim, D. J.; Caruthers, J. M.; Peppas, N. A. *Chem. Eng. Sci.* **1996,** 51, (21), 4827-4841.